Acta Crystallographica Section C
Crystal Structure Communications
ISSN 0108-2701

Two transition metal coordination polymers of the 7,7,8,8-tetracyanoquinodimethane dianion ($TCNQ^{2-}$)

Guangbin Wang, Carla Slebodnick and Gordon T. Yee*

Department of Chemistry, Virginia Polytechnic Institute and State University, Blacksburg, VA 24061, USA
Correspondence e-mail: gyee@vt.edu

Received 30 October 2008
Accepted 5 December 2008
Online 17 December 2008

Each of the two novel title transition metal coordination polymers, namely *catena*-poly[[bis{[tris(2-pyridylmethyl)amine]-cobalt(II)}-μ_4-7,7,8,8-tetracyanoquinodimethanide(2−)] bis-[7,7,8,8-tetracyanoquinodimethanide(1−)] methanol disolvate], $\{[Co_2(C_{12}H_4N_4)(C_{18}H_{18}N_4)_2](C_{12}H_4N_4)_2\cdot 2CH_3OH\}_n$, (I), and *catena*-poly[[[[tris(2-pyridylmethyl)amine]iron(II)]-μ_2-7,7,8,8-tetracyanoquinodimethanide(2−)] methanol solvate], $\{[Fe(C_{12}H_4N_4)(C_{18}H_{18}N_4)]\cdot CH_3OH\}_n$, (II), contains η^4-TPA and *cis*-bridging $TCNQ^{2-}$ ligands [TPA is tris(2-pyridylmethyl)amine and TCNQ is 7,7,8,8-tetracyanoquinodimethane], but the two compounds adopt entirely different structural motifs. Compound (I) consists of a ribbon coordination polymer featuring μ_4-$TCNQ^{2-}$ radical anion ligands bridging four different octahedral Co^{II} centers. Each formula unit of the polymer is flanked by two uncoordinated $TCNQ^-$ anions and two methanol solvent molecules. All three TCNQ anions have crystallographic inversion symmetry. In (II), the 2_1 symmetry operator generates a one-dimensional zigzag chain of octahedral Fe^{II} centers with μ_2-$TCNQ^{2-}$ bridges. A methanol solvent molecule forms hydrogen bonds to one of the terminal N atoms of the bridging $TCNQ^{2-}$ dianion. To the best of our knowledge, these are the first examples of one-dimensional coordination polymers forming from *cis* coordination of two TCNQ ligands to octahedral metal centers.

Comment

The ability of 7,7,8,8-tetracyanoquinodimethane anions ($TCNQ^{n-}$, n = 1 or 2) to coordinate to transition metal fragments and to act as bridging σ-donor ligands (μ_2, μ_3, or μ_4) can be exploited to construct extended molecular assemblies. Interest in this area has been spurred, in part, by several observations of long-range magnetic order in $TCNQ^-$-bridged structures involving V, Mn, Fe, Co, and Ni ions (Vickers *et al.*, 2004, 2005; Clérac *et al.*, 2003). A review of this area includes descriptions of the various modes of coordination, as well as compilations of IR, X-ray, and electrochemical data (Kaim & Moscherosch, 1994).

For the case when exactly two TCNQ ligands coordinate to an octahedral metal center, a search of the Cambridge Structural Database (Version 5.29; Allen, 2002) using *CONQUEST* (Macrae *et al.*, 2006) indicates a preference for *trans* TCNQ coordination to the metal center (Kunkeler *et al.*, 1996; Cornelissen *et al.*, 1992; Oshio *et al.*, 1995; Azcondo *et al.*, 1996; Sugiura *et al.*, 1999; Choi & Suh, 2003; Ballester, Gil *et al.*, 1997; Ballester, Gutiérrez *et al.*, 1997; Ballester *et al.*, 1994, 2002, 2004). In this context, *trans* and *cis* refer to the relative geometry of two ligands about a single metal center, and *syn*, *anti* and *gem* describe the three possible μ_2-bridging geometries of the TCNQ ligand. Additionally, there are examples of four TCNQ ligands or TCNQ–TCNQ σ-dimers coordinated equatorially to an octahedral metal center to form $M(L_2)(TCNQ)_4$ or $ML_2(TCNQ)_2(TCNQ\text{–}TCNQ)_2$ (Zhao *et al.*, 1999; Shimomura *et al.*, 2006). These complexes form coordination polymers, three *via* μ_2-TCNQ bridging (two *gem* and one *syn*) and one *via* μ_4-TCNQ bridging. To the best of our knowledge, there is only one example of *cis* geometry when only two TCNQ ligands are coordinated to an octahedral metal center (Ballester, Gutiérrez *et al.*, 1997) and no examples that give rise to pseudo-one-dimensional coordination polymers, as occur in the title compounds, (I) and (II).

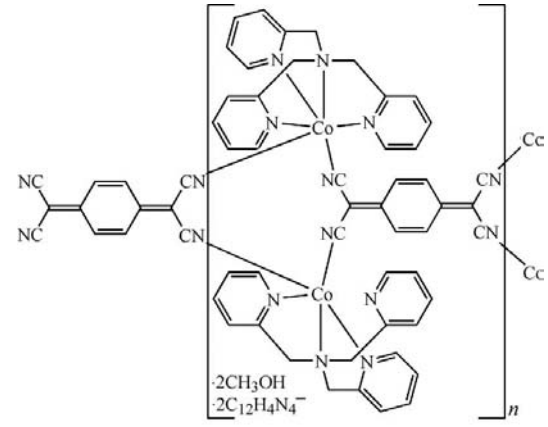

(I)

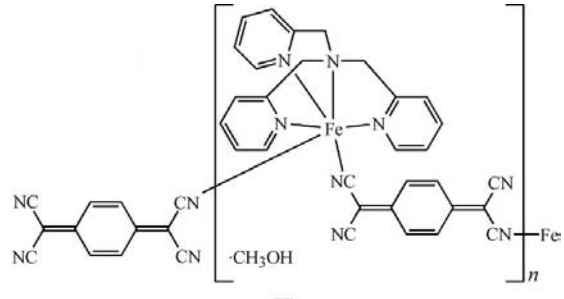

(II)

The μ_4-bridging mode is also relatively rare, though not unprecedented. The discrete complex $[(\mu_4\text{-TCNQ})\{fac\text{-}Re(CO)_3(bpy)\}_4]^{4+}$ has been formulated to contain neutral TCNQ (Hartmann *et al.*, 2001). The compounds $[\{M_2(O_2C\text{-}CF_3)_4\}_2(\mu_4\text{-TCNQ})\cdot 3(solvate)]_\infty$ (M = Rh, Ru or Mo) are

  doi:10.1107/S0108270108041152

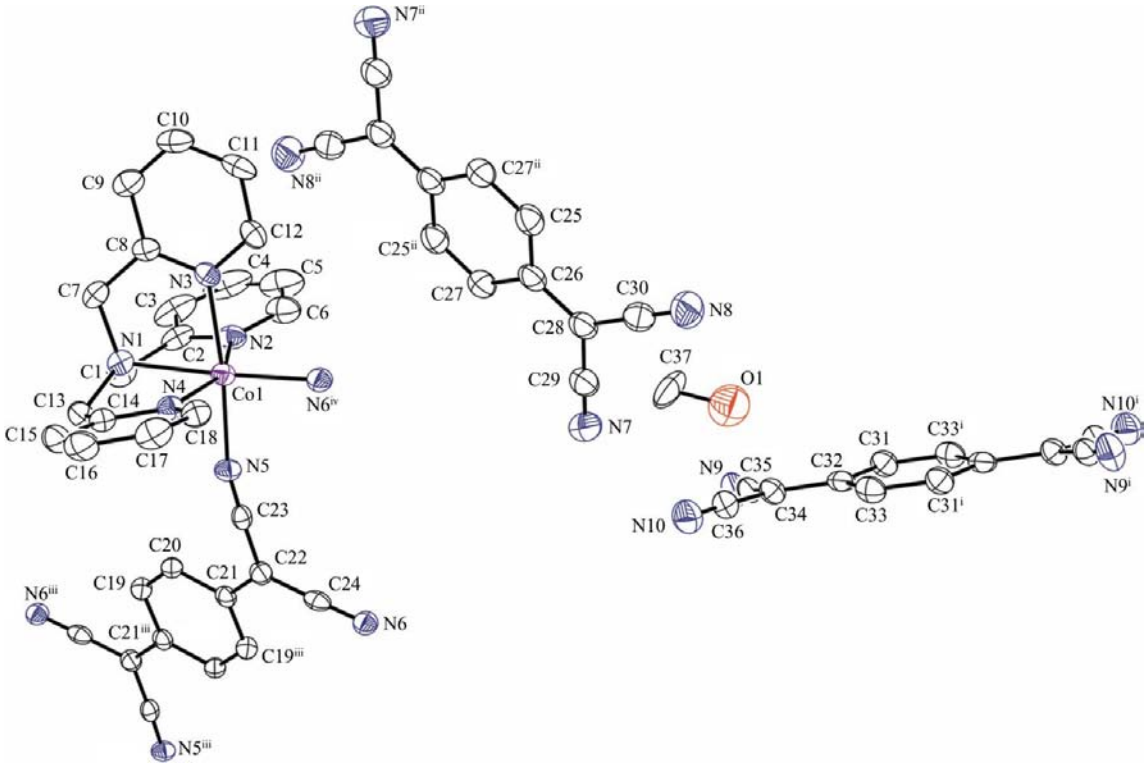

Figure 1
A view of the asymmetric unit of (I), showing the atom-numbering scheme. Displacement ellipsoids are drawn at the 50% probability level and H atoms have been omitted for clarity. [Symmetry codes: (i) $-x, -y+1, -z$; (ii) $-x+1, -y+1, -z+1$; (iii) $-x, -y+3, -z+1$; (iv) $-x, -y+2, -z+1$.]

reported to contain partially reduced, but formally neutral, bridging TCNQ (Miyasaka *et al.*, 2000, 2006; Campana *et al.*, 1996). The ends of each $\{M_2(O_2CCF_3)_4\}_2$ 'barrel' are coordinated by two TCNQ ligands to give either a one-dimensional chain (Mo) or two-dimensional sheets (Rh and Ru). In contrast, $[Ag(\mu_4\text{-TCNQ})]_\infty$ (Shields, 1985) and a Cu analog (Heintz *et al.*, 1999) possess the ligand in the radical anionic state and form three-dimensional structures comprised of two interpenetrating networks. Shimomura *et al.* (2006) have reported a porous framework consisting of Zn^{II} ions bridged by μ_4-$TCNQ^{2-}$ to form corrugated sheets that are connected by 4,4′-bipyridine pillars. Most relevant to the present work, $[Mn^{III}(salen)(\mu_4\text{-TCNQ})_{0.5}][Mn^{III}(salen)(\mu_2\text{-TCNQ})_{0.5}(CH_3OH)]$ [H_2salen is bis(salicylidene)ethylenediamine] contains two crystallographically independent TCNQs, one *anti*-μ_2-$TCNQ^{2-}$ and one μ_4-bridging (Oshio *et al.*, 1995).

Our original goal was to exploit the bridging propensity and radical property of $TCNQ^-$ to prepare discrete magnetic molecular squares with octahedral transition metal complexes as the corners and radical anions as the edges. One reason for this line of research was to prepare nanoscale fragments of the above-mentioned magnetically ordered phases. To achieve this, we chose the tripodal tetradentate ligand tris(2-pyridylmethyl)amine (TPA) to cap four of the available coordination sites, leaving two *cis* sites on each metal center open for the $TCNQ^-$ binding necessary to close the square. Oshio *et al.* (1993) have previously reported an $[Mn(TPA)(TCNQ)(CH_3OH)]$ complex in which the $N_{TCNQ}-Mn-O$ angle is 90.5°, seemingly ideal for our goal of coordinating two *cis*-TCNQ anions to form a corner building block.

Unfortunately, our first efforts in this area have not yielded the desired squares. Instead, we have discovered that LiTCNQ reacts with Fe^{II}TPA and Co^{II}TPA complexes to give magnetically unremarkable but structurally interesting coordination polymers. In each case, a known reaction occurs involving disproportionation of two TCNQ radical anions to yield the diamagnetic $TCNQ^{2-}$ (Grossel *et al.*, 2000). Although the goal of synthesizing molecular squares was not met, it is gratifying to see two $TCNQ^{2-}$ dianions coordinated *cis* to each metal center, as would be required for square construction.

The asymmetric unit of (I) comprises one Co(TPA)-$(TCNQ)_{0.5}$ formula unit, two uncoordinated $0.5TCNQ^-$ located on inversion centers, and one methanol solvent molecule (Fig. 1). The Co^{II} ion adopts a distorted octahedral geometry, with the TPA ligand occupying four coordination sites and two *cis*-coordinated $TCNQ^{2-}$ ligands occupying the remaining two sites. The Co—N bond lengths (Table 1) are all within expected ranges (Allen, 2002; Macrae *et al.*, 2006). The coordinated $TCNQ^{2-}$ ligand adopts a μ_4-bridging mode to four different Co atoms, forming an infinite ribbon (Fig. 2). The nonbonded $TCNQ^-$ anions and methanol solvent molecules flank the ribbon on all sides. One of these nonbonded $TCNQ^-$ anions is nearly parallel with the μ_4-$TCNQ^{2-}$ ligand [dihedral angle = 2.05 (12)°; Fig. 3, $TCNQ^-$ *B*] and the other $TCNQ^-$ anion is nearly parallel with the pyridyl group of the TPA ligand [dihedral angle = 7.83 (19)°; Fig. 3, $TCNQ^-$ *A*].

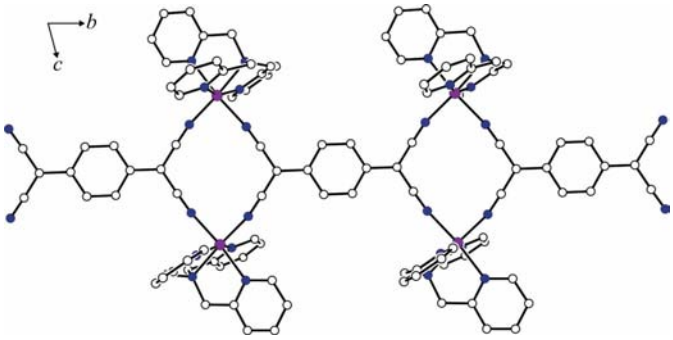

Figure 2
A view of the structure of (I) down the *a** direction, showing the one-dimensional ribbon architecture. The methanol solvent molecules and uncoordinated $TCNQ^{-}$ anions have been omitted for clarity.

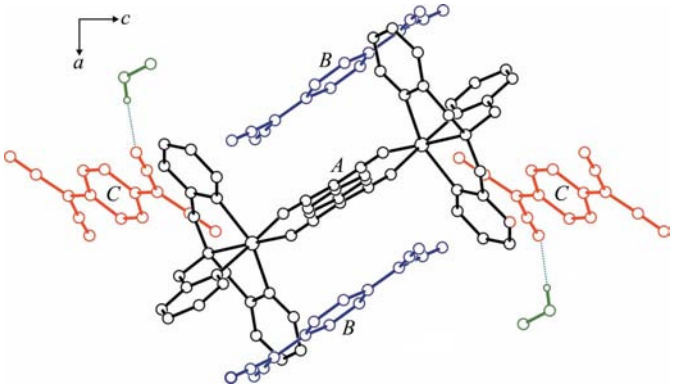

Figure 3
A view of (I) down the *b* axis, illustrating the hydrogen bonding (dotted lines) with the methanol molecules and the packing of the uncoordinated $TCNQ^{-}$ anions.

The hydroxy group of the methanol is hydrogen bonded to an N atom of a nonbonded $TCNQ^{-}$ (Table 2). For charge balance, the three TCNQ entities in the formula unit must have a total charge of −4. The formal charges of −2 for the μ_4-TCNQ and −1 for the two uncoordinated TCNQs are assigned based on the C—C bond lengths observed in the crystal structure (see below).

The asymmetric unit of (II) comprises one Fe(TPA)(TCNQ) unit and one methanol solvent molecule (Fig. 4). The Fe^{II} ion adopts a distorted octahedral geometry, with a tetradentate TPA ligand and two *cis*-coordinated $TCNQ^{2-}$ coordinated to the metal. The Fe—N bond lengths (Table 3) are typical of other Fe^{II} low-spin TPA complexes (Allen, 2002; Macrae *et al.*, 2006). Each μ_2-$TCNQ^{2-}$ ligand adopts an *anti* bridging mode to form a zigzag chain propagating along the crystallographic *b* axis (Fig. 5). The infinite chain is generated by a 2_1 screw axis at $(\frac{1}{2}, y, \frac{1}{4})$ (origin at $\overline{1}$) and neighboring chains are related by inversion symmetry. The hydroxy group of the methanol solvent molecule is hydrogen bonded to a free N atom of the $TCNQ^{2-}$ (Fig. 5 and Table 4).

X-ray crystallography can be used to confirm the oxidation states of the TCNQ species in these materials. Successive reduction of TCNQ leads to a progressive and characteristic

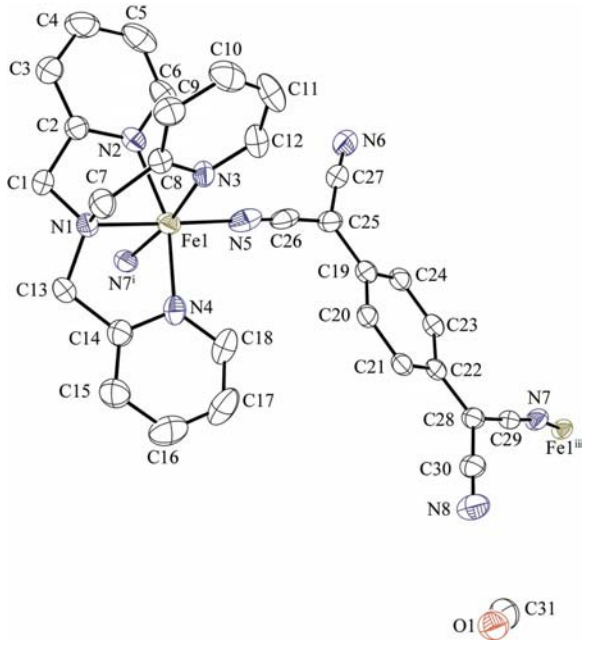

Figure 4
A view of the asymmetric unit of (II), showing the atom-numbering scheme. Displacement ellipsoids are drawn at the 50% probability level and H atoms have been omitted for clarity. [Symmetry codes: (i) $-x+1, y-\frac{1}{2}, -z+\frac{1}{2}$; (ii) $-x+1, y+\frac{1}{2}, -z+\frac{1}{2}$.]

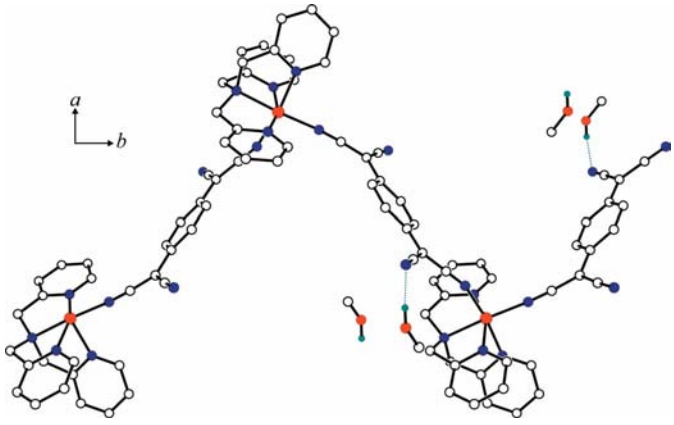

Figure 5
A view of (II) down the *c* axis, showing the one-dimensional zigzag chain architecture and the hydrogen bonding (dotted lines) with the methanol molecules.

increase in benzoid character in the six-membered ring and a lengthening of the exocyclic C—C bonds (Fig. 6) (Zhao *et al.*, 1996; Miyasaka *et al.*, 2000). Table 5 lists selected intramolecular bond distances for the TCNQ anions in complexes (I) and (II), as well as typical values for TCNQ, $TCNQ^{-}$ and $TCNQ^{2-}$. In (I), there are three unique TCNQ anions, denoted *A*, *B* and *C* (Fig. 3). The bond lengths in TCNQ *A*, which is coordinated to Co^{II} in a μ_4-bridging mode, are consistent with $TCNQ^{2-}$. The bond lengths in the uncoordinated anions *B* and *C* are consistent with $TCNQ^{-}$. These oxidation state assignments give a total charge of −4 to

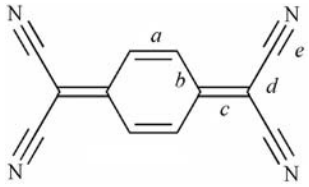

Figure 6
The bond labeling used in Table 5.

balance the +2 charge of the two Co^{II} ions and give an empirical formula of $[Co_2^{II}(\mu_4\text{-}TCNQ^{2-})(TPA)_2](TCNQ^-)_2\cdot 2CH_3OH$. In (II), the bond lengths in the one crystallographically independent TCNQ anion indicate a charge of −2, which balances the +2 charge of the Fe^{II} cation and gives an empirical formula of $[Fe^{II}(\mu_2\text{-}TCNQ^{2-})(TPA)]\cdot CH_3OH$.

Experimental

Hazard warning: Perchlorate salts are potentially explosive and should be used in small amounts and handled with care (Wolsey, 1973). Preparations of air-sensitive compounds were carried out in a nitrogen-filled Vacuum Atmospheres glove-box using standard Schlenk techniques. Reagents were used as received except as noted below. Solvents were distilled from the appropriate drying agent under nitrogen: dichloromethane and acetonitrile were distilled from P_2O_5, diethyl ether was distilled from Na/benzophenone, and methanol was distilled from Na. All solvents were degassed with glove-box N_2 prior to use. Tris(2-pyridylmethyl)amine and $[Fe(TPA)(CH_3CN)_2](ClO_4)_2$ were prepared according to literature procedures (Karlin *et al.*, 1982; Zang *et al.*, 1993, 1997). LiTCNQ was prepared by adding a boiling solution of LiI (400 mg, 3 mmol) in acetonitrile (20 ml) to a boiling solution of TCNQ (210 mg, 1.0 mmol) in acetonitrile (200 ml). A dark-purple precipitate was collected by suction (Bozio *et al.*, 1975). IR spectra were measured using a MIDAC *M*-series FT–IR spectrometer equipped with an ATR attachment. Elemental analyses were performed by Desert Analytics, Tucson, Arizona.

For the preparation of (I), a solution of LiTCNQ (42.2 mg, 0.200 mmol) in methanol (3 ml) was added to a mixture of $Co(NO_3)_2\cdot 6H_2O$ (29.1 mg, 0.100 mmol) and TPA (29.0 mg, 0.100 mmol) in methanol (4 ml). The mixture was stirred for 3 h at room temperature, and the blue–black precipitate that formed was filtered off, washed with methanol and ether, and dried *in vacuo*. Dark-green plates of (I) were crystallized from methanol–diethyl ether by vapor diffusion at room temperature (yield 7.0 mg, 10%). Analysis calculated for $C_{37}H_{28}CoN_{10}O$: C 64.63, H 4.10, N 20.34%; found: C 64.77, H 3.89, N 20.44%. IR (ν, cm^{-1}): 2188, 2176, 2140, 2059, 824.

For the preparation of (II), the red solid $[Fe(TPA)(CH_3CN)_2](ClO_4)_2$ (62.7 mg, 0.100 mmol) was dissolved in CH_2Cl_2 (6 ml) to yield a yellow solution. A green solution of LiTCNQ (42.2 mg, 0.200 mmol) in CH_3OH (6 ml) was added, leading to a deep-green solution. The solution was stirred for 3 h at room temperature and a dark-blue solid was filtered off, washed with methanol and ether, and dried *in vacuo*. Dark-orange bricks of (II) were crystallized from methanol–diethyl ether by vapor diffusion at room temperature (yield 6.2 mg, 11%). Analysis calculated for $C_{31}H_{26}FeN_8O$: C 63.93, H 4.50, N 19.24%; found: C 64.01, H 3.50, N 20.50%. IR (ν, cm^{-1}): 2187, 2180, 2155, 2106, 822.

Compound (I)

Crystal data

$[Co_2(C_{12}H_4N_4)(C_{18}H_{18}N_4)_2](C_{12}H_4N_4)_2\cdot 2CH_4O$
M_r = 1375.24
Triclinic, $P\overline{1}$
a = 8.954 (2) Å
b = 11.371 (3) Å
c = 17.066 (4) Å
α = 73.45 (2)°
β = 85.55 (2)°
γ = 74.93 (2)°
V = 1608.3 (7) Å^3
Z = 1
Mo $K\alpha$ radiation
μ = 0.58 mm^{-1}
T = 100 (2) K
0.14 × 0.11 × 0.03 mm

Data collection

Oxford Diffraction Xcalibur diffractometer
11614 measured reflections
5716 independent reflections
3386 reflections with $I > 2\sigma(I)$
R_{int} = 0.046

Refinement

$R[F^2 > 2\sigma(F^2)]$ = 0.047
$wR(F^2)$ = 0.105
S = 0.86
5716 reflections
444 parameters
H-atom parameters constrained
$\Delta\rho_{max}$ = 0.47 e Å^{-3}
$\Delta\rho_{min}$ = −0.51 e Å^{-3}

Compound (II)

Crystal data

$[Fe(C_{12}H_4N_4)(C_{18}H_{18}N_4)]\cdot CH_4O$
M_r = 582.45
Monoclinic, $P2_1/c$
a = 9.4197 (10) Å
b = 18.2526 (18) Å
c = 17.0040 (18) Å
β = 105.275 (9)°
V = 2820.3 (5) Å^3
Z = 4
Mo $K\alpha$ radiation
μ = 0.58 mm^{-1}
T = 100 (2) K
0.14 × 0.12 × 0.10 mm

Data collection

Oxford Diffraction Xcalibur diffractometer
15228 measured reflections
5257 independent reflections
3180 reflections with $I > 2\sigma(I)$
R_{int} = 0.036

Table 1
Selected bond lengths (Å) for (I).

Co1—N6^{i}	2.019 (3)	Co1—N2	2.124 (3)
Co1—N5	2.113 (3)	Co1—N3	2.129 (3)
Co1—N4	2.122 (3)	Co1—N1	2.164 (3)

Symmetry code: (i) $-x, -y+2, -z+1$.

Table 2
Hydrogen-bond geometry (Å, °) for (I).

D—H···A	D—H	H···A	D···A	D—H···A
O1—H1···N9	0.84	1.99	2.829 (5)	172

Table 3
Selected bond lengths (Å) for (II).

Fe1—N5	1.996 (3)	Fe1—N2	2.0767 (19)
Fe1—N7^{i}	2.000 (2)	Fe1—N4	2.077 (2)
Fe1—N3	2.0611 (19)	Fe1—N1	2.0987 (18)

Symmetry code: (i) $-x+1, y-\frac{1}{2}, -z+\frac{1}{2}$.

Refinement

$R[F^2 > 2\sigma(F^2)] = 0.037$	372 parameters
$wR(F^2) = 0.086$	H-atom parameters constrained
$S = 0.84$	$\Delta\rho_{max} = 0.59$ e Å^{-3}
5257 reflections	$\Delta\rho_{min} = -0.22$ e Å^{-3}

Table 4
Hydrogen-bond geometry (Å, °) for (II).

D—H···A	D—H	H···A	D···A	D—H···A
O1—H1···N8	0.84	2.07	2.889 (3)	166

Table 5
Intramolecular bond distances (Å) for the TCNQ species in (I) and (II).

Species	*a*	*b*	*c*	*d*	*e*
TCNQ†	1.345	1.448	1.374	1.441	1.140
$TCNQ^-$†	1.374	1.423	1.420	1.416	1.153
$TCNQ^{2-}$†	1.380 (9)	1.395 (9)	1.4919 (9)	1.392 (9)	1.167 (9)
$TCNQ^{2-}$ *A* in (I)	1.375 (4)	1.383 (4)	1.476 (4)	1.405 (4)	1.156 (4)
		1.403 (4)		1.386 (5)	1.164 (4)
$TCNQ^-$ B in (I)	1.357 (5)	1.414 (5)	1.417 (5)	1.410 (5)	1.154 (5)
		1.420 (5)		1.420 (5)	1.149 (4)
$TCNQ^-$ C in (I)	1.363 (5)	1.410 (4)	1.419 (4)	1.409 (5)	1.153 (4)
		1.418 (4)		1.422 (5)	1.152 (4)
$TCNQ^{2-}$ in (II)	1.384 (3)	1.401 (3)	1.468 (3)	1.416 (4)	1.155 (3)
	1.386 (3)	1.402 (3)	1.471 (3)	1.402 (4)	1.158 (3)
		1.395 (3)		1.397 (3)	1.156 (3)
		1.393 (3)		1.397 (3)	1.157 (3)

† References: Zhao *et al.* (1996); Miyasaka *et al.* (2000).

H atoms were treated using a riding model, with aromatic C—H = 0.95 Å and U_{iso}(H) = 1.2U_{eq}(C), methylene C—H = 0.99 Å and U_{iso}(H) = 1.2U_{eq}(C) and methyl C—H = 0.98 Å and U_{iso}(H) = 1.5U_{eq}(C). The hydroxy H atoms were located in a difference map and subsequently treated as riding, with O—H = 0.84 Å and U_{iso}(H) = 1.5U_{eq}(O).

For both compounds, data collection: *CrysAlisPro* (Oxford Diffraction, 2007); cell refinement: *CrysAlisPro*; data reduction: *CrysAlisPro*. Program(s) used to solve structure: *SHELXS86* (Sheldrick, 2008) and *WinGX* (Farrugia, 1999) for (I); *SHELXS97* (Sheldrick, 2008) for (II). For both compounds, program(s) used to refine structure: *SHELXL97* (Sheldrick, 2008); molecular graphics: *SHELXTL*/*NT* (Sheldrick, 2008); software used to prepare material for publication: *SHELXTL*/*NT* (Sheldrick, 2008).

The authors gratefully acknowledge the National Science Foundation (grant Nos. CHE-0518220 and CHE-0131128) for funding this research and the purchase of the Oxford Diffraction Xcalibur S single-crystal diffractometer, respectively.

Supplementary data for this paper are available from the IUCr electronic archives (Reference: SQ3174). Services for accessing these data are described at the back of the journal.

References

Allen, F. H. (2002). *Acta Cryst.* B**58**, 380–388.
Azcondo, M. T., Ballester, L., Gutierrez, A., Perpinan, M. F., Amador, U., Ruiz-Valero, C. & Bellitto, C. (1996). *J. Chem. Soc. Dalton Trans.* pp. 3015–3019.
Ballester, L., Barral, M. C., Gutierrez, A., Monge, A., Perpinan, M. F., Ruiz-Valero, C. & Sanchez-Pelaez, A. E. (1994). *Inorg. Chem.* **33**, 2142–2146.
Ballester, L., Gil, A. M., Gutiérrez, A., Perpiñán, M. F., Azcondo, M. T., Sánchez, A. E., Amador, U., Campo, J. & Palacio, F. (1997). *Inorg. Chem.* **36**, 5291–5298.
Ballester, L., Gil, A. M., Gutiérrez, A., Perpiñán, M. F., Azcondo, M. T., Sánchez, A. E., Marzin, C., Tarrago, G. & Bellitto, C. (2002). *Chem. Eur. J.* **8**, 2539–2548.
Ballester, L., Gutiérrez, A., Perpiñán, M. F., Amador, U., Azcondo, M. T., Sánchez, A. E. & Bellitto, C. (1997). *Inorg. Chem.* **36**, 6390–6396.
Ballester, L., Gutiérrez, A., Perpiñán, M. F., Sánchez, A. E., Azcondo, M. T. & González, M. J. (2004). *Inorg. Chim. Acta*, **357**, 1054–1062.
Bozio, R., Girlando, A. & Pecile, C. (1975). *J. Chem. Soc. Faraday Trans. 2*, **71**, 1237–1254.
Campana, C. F., Dunbar, K. R. & Ouyang, X. (1996). *Chem. Commun.* pp. 2427–2428.
Choi, H. J. & Suh, M. P. (2003). *Inorg. Chem.* **42**, 1151–1157.
Clérac, R., O'Kane, S., Cowen, J., Ouyang, X., Heintz, R., Zhao, H., Bazile, M. J. Jr & Dunbar, K. R. (2003). *Chem. Mater.* **15**, 1840–1850.
Cornelissen, J. P., van Diemen, J. H., Groeneveld, L. R., Haasnoot, J. G., Spek, A. L. & Reedijk, J. (1992). *Inorg. Chem.* **31**, 198–202.
Farrugia, L. J. (1999). *J. Appl. Cryst.* **32**, 837–838.
Grossel, M. C., Duke, A. J., Hibbert, D. B., Lewis, I. K., Seddon, E. A., Horton, P. N. & Weston, S. C. (2000). *Chem. Mater.* **12**, 2319–2323.
Hartmann, H., Kaim, W., Hartenbach, I., Schleid, T., Wanner, M. & Fiedler, J. (2001). *Angew. Chem. Int. Ed.* **40**, 2842–2844.
Heintz, R. A., Zhao, H., Ouyang, X., Grandinetti, G., Cowen, J. & Dunbar, K. R. (1999). *Inorg. Chem.* **38**, 144–156.
Kaim, W. & Moscherosch, M. (1994). *Coord. Chem. Rev.* **129**, 157–193.
Karlin, K. D., Hayes, J. C., Juen, S., Hutchinson, J. P. & Zubieta, J. (1982). *Inorg. Chem.* **21**, 4106–4108.
Kunkeler, P. J., van Koningsbruggen, P. J., Cornelissen, J. P., van der Horst, A. N., van der Kraan, A. M., Spek, A. L., Haasnoot, J. G. & Reedijk, J. (1996). *J. Am. Chem. Soc.* **118**, 2190–2197.
Macrae, C. F., Edgington, P. R., McCabe, P., Pidcock, E., Shields, G. P., Taylor, R., Towler, M. & van de Streek, J. (2006). *J. Appl. Cryst.* **39**, 453–457.
Miyasaka, H., Campos-Fernández, C. S., Clérac, R. & Dunbar, K. R. (2000). *Angew. Chem. Int. Ed.* **39**, 3831–3835.
Miyasaka, H., Izawa, T., Takahashi, N., Yamashita, M. & Dunbar, K. R. (2006). *J. Am. Chem. Soc.* **128**, 11358–11359.
Oshio, H., Ino, E., Ito, T. & Maeda, Y. (1995). *Bull. Chem. Soc. Jpn*, pp. 889–897.
Oshio, H., Ino, E., Ito, T., Mogi, I. & Ito, T. (1993). *Inorg. Chem.* **32**, 5697–5703.
Oxford Diffraction (2007). *CrysAlisPro*. Version 171.32. Oxford Diffraction Ltd, Abingdon, England.
Sheldrick, G. M. (2008). *Acta Cryst.* A**64**, 112–122.
Shields, L. (1985). *J. Chem. Soc. Faraday Trans. 2*, **81**, 1–9.
Shimomura, S., Matsuda, R., Tsujino, T., Kawamura, T. & Kitagawa, S. (2006). *J. Am. Chem. Soc.* **128**, 16416–16417.
Sugiura, K., Mikami, S., Johnson, M. T., Miller, J. S., Iwasaki, K., Umishita, K., Hino, S. & Sakata, Y. (1999). *Chem. Lett.* pp. 925–926.
Vickers, E. B., Giles, I. D. & Miller, J. S. (2005). *Chem. Mater.* **17**, 1667–1672.
Vickers, E. B., Selby, T. D., Thorum, T. S., Taliaferro, M. L. & Miller, J. S. (2004). *Inorg. Chem.* **43**, 6414–6420.
Wolsey, W. C. (1973). *J. Chem. Educ.* **50**, A335–A337.
Zang, Y., Elgren, T. E., Dong, Y. & Que, L. Jr (1993). *J. Am. Chem. Soc.* **115**, 811–813.
Zang, Y., Kim, J., Dong, Y., Wilkinson, E. C., Appelman, E. H. & Que, L. Jr (1997). *J. Am. Chem. Soc.* **119**, 4197–4205.
Zhao, H., Heintz, R. A. & Dunbar, K. R. (1996). *J. Am. Chem. Soc.* **118**, 12844–12845.
Zhao, H., Heintz, R. A., Ouyang, X., Dunbar, K. R., Campana, C. F. & Rogers, R. D. (1999). *Chem. Mater.* **11**, 736–746.